AJNR

Detection of Intracranial Hemorrhage: Comparison between Gradient-echo Images and b_0 Images Obtained from Diffusion-weighted Echo-planar Sequences

Doris D. M. Lin, Christopher G. Filippi, Alex B. Steever and Robert D. Zimmerman

Detection of Intracranial Hemorrhage: Comparison between Gradient-echo Images and b_0 Images Obtained from Diffusion-weighted Echo-planar Sequences

Doris D. M. Lin, Christopher G. Filippi, Alex B. Steever, and Robert D. Zimmerman

BACKGROUND AND PURPOSE: **Diffusion-weighted MR imaging (DWI) is commonly used as the initial and sole imaging examination for the detection of acute cerebral infarction, yet it remains controversial whether MR can detect hyperacute (<24 h) hemorrhage. Hemorrhage is best detected with gradient-echo (GRE) T2*-weighted sequences, because of their magnetic susceptibility effects. DWI uses a spin-echo echo-planar technique (EPI) that is more sensitive than spin-echo T2-weighted imaging to susceptibility effects. Our aim was to determine whether the b_0 image from the DWI-EPI sequence is as sensitive as GRE in detecting hemorrhagic lesions on imaging studies performed to identify acute infarction or hemorrhage.**

METHODS: **All MR studies performed for clinically suspected or radiographically confirmed acute infarction or hemorrhage from 2/1/98 to 8/15/99 were retrospectively interpreted by one neuroradiologist in a blinded fashion. The sensitivity of hemorrhage detection, conspicuity of lesions, and diagnostic certainty were compared between the b_0 EPI and GRE sequences.**

RESULTS: **We found 101 acute infarcts, of which 13 were hemorrhagic, as evidenced by the presence of hypointensity within the infarction on the GRE sequence. This finding served as the reference standard for detection of hemorrhage. Hemorrhage was diagnosed with confidence in only seven cases (54%) on b_0 images; 22 acute hematomas were hypointense on GRE images whereas 19 were hypointense on b_0 images (86%); 17 chronic hematomas were depicted on GRE images and 12 on b_0 scans (63%). Punctate hemorrhages and linear cortical staining were detected on 37 GRE studies but on only four b_0 studies. Hemorrhage was always more conspicuous on the GRE sequences.**

CONCLUSION: **b_0 images from a DWI sequence failed to detect minimally hemorrhagic infarctions and small chronic hemorrhages associated with microangiopathy. GRE scans were more sensitive than b_0 images in the detection of these hemorrhages and should be included in emergency brain MR studies for acute infarction, especially when thrombolytic therapy is contemplated.**

Diagnosis and management of cerebral infarction have been revolutionized by the development of diffusion-weighted imaging (DWI) performed with an echo-planar (EPI) technique. Hyperacute cerebral infarction can be detected in experimental animal studies within minutes of ictus (1), and, in clinical practice, it can be accurately diagnosed with confidence within hours of the onset of neurologic symptoms (2, 3). The sensitivity of MR imaging with DWI surpasses that of CT. New treatment options (eg, thrombolytic and neuroprotective agents) have been introduced, but their effectiveness is critically dependent on the ability to detect and determine the extent of infarction and to exclude hemorrhage within the first few hours. It is, therefore, not surprising that emergency brain MR imaging is assuming an increasingly important role and has been recommended to replace CT for screening acute cerebral infarction (4).

In thrombolytic therapy, it is critical to identify the presence of concomitant hemorrhage, in which case the risk of treatment (ie, massive hemorrhage) outweighs the therapeutic benefit. In general, unenhanced CT provides quick, easily accessible, and accurate assessment of various forms of intracranial hemorrhage, and has been used in numerous

trial studies as the imaging method by which to select patients who may benefit from thrombolysis. The effectiveness of conventional MR imaging in the assessment of acute hemorrhage has been questioned in the past, but a number of studies have indicated that gradient-echo (GRE) and fluid-attenuated inversion-recovery (FLAIR) sequences markedly increase the sensitivity of MR imaging (5–9) as compared with older MR sequences and CT. Use of MR imaging to investigate acute parenchymal and intraventricular hemorrhage in a dog model showed that GRE was more sensitive than conventional spin-echo T1- and T2-weighted sequences in depicting hyperacute hemorrhage (10). Hypointensity on GRE images appeared within 1 hour of hematoma production. GRE was also superior to CT in detection of these hemorrhages (10). In another study, which compared findings from an animal model with clinical examinations, intracerebral hematoma of less than 24 hours' duration was shown to have a characteristic hypointense rim surrounding variable, heterogeneous hyperintensity on T2-weighted spin-echo images (11). This rim of hypointensity on T2-weighted sequences resulted from intravoxel dephasing that demarcated a transition from a fully oxygenated to a fully deoxygenated hematoma and that with time moved from the periphery to the core of the lesion. More diffuse signal loss (hypointensity) throughout the lesion could be identified on GRE images owing to their greater sensitivity to magnetic susceptibility. This feature is exploited in susceptibility-weighted imaging sequences (T2*-weighted GRE and EPI sequences), which provide superior sensitivity in detecting hemorrhage as compared with spin-echo sequences. Furthermore, in clinical as well as in vivo animal models, use of these susceptibility-weighted sequences has been confirmed to provide sensitivity and accuracy equal to or greater than that of CT (8, 12).

In routine clinical DWI, four sets of spin-echo EPI images are acquired. Three DWI sets (obtained with orthogonally applied diffusion gradients) are combined to produce an isotropic DWI scan, and a b_0 set is acquired without diffusion gradients. Since EPI is intrinsically sensitive to magnetic field inhomogeneity, paramagnetic blood breakdown products produce signal loss similar to that in T2*-weighted GRE sequence. In theory, the b_0 image may thus be helpful in identifying hemorrhagic infarction without the need for extra scanning time. Ebisu et al (13) reported the utility of diffusion- and T2-weighted spin-echo EPI (ie, b_0 image) in detecting and distinguishing between hemorrhagic and nonhemorrhagic acute and subacute infarction. Acute hemorrhagic infarction could be discriminated on the basis of T2-weighted EPI, in which the signal intensity of the lesion was significantly lower than that of the nonhemorrhagic infarction (increased signal intensity). The reduction in signal was attributed to T2* effects. On the other hand, Linfante et al (14) asserted that DWI was less specific in the diagnosis of hemorrhage than in defining ischemia, and that EPI GRE sequences (ie, EPI/T2*-weighted) offered the most useful means of detecting signal changes in hyperacute hemorrhage within 2 hours of onset.

In devising a fast MR protocol for acute stroke, we have included sagittal T1-weighted, axial T2-weighted, FLAIR, and DWI sequences, which take less than 7 minutes to acquire. The b_0 image always comes with DWI; therefore, it imposes no additional time and may serve as both T2- and susceptibility-weighted images. If a routine GRE sequence were included, 2 to 3 minutes (setup plus 1:45 minutes scan time) would be added to the examination time.

In this study we tested the hypothesis that the b_0 image from DWI spin-echo EPI can be used to depict hemorrhagic lesions as effectively as the T2*-weighted GRE sequence, thereby eliminating the need to perform an additional GRE sequence to detect acute hemorrhage.

Methods

All MR studies performed in our institution between 2/1/98 and 8/15/99 for clinically suspected or radiographically identified acute infarction or hemorrhage (<4 days old) were included in this study. These examinations were performed using a 1.5-T MR unit with echo-planar capability. DWI spin-echo EPI (10,000/102/1 [TR/TE/excitations], 128 × 128 matrix, 40-second acquisition time) with orthogonally applied (*x, y,* and *z* axes) diffusion gradients was performed with a b value of 1000. These three images were combined to produce an isotropic DWI scan. A separate image was acquired without the diffusion gradients (the b_0 image). An axial GRE sequence (425/15/1, 20° flip angle, 256 × 160 matrix, 1:45-minute acquisition time) was acquired in all cases, as were routine sagittal T1-weighted spin-echo (500/12/1, 1:20-minute acquisition time), axial T2-weighted fast spin-echo (3000/82/1, 42-second acquisition time), and FLAIR (10002/162/1, 3:20-minute acquisition time) sequences.

In each case the b_0 EPI and GRE images were independently reviewed in conjunction with the isotropic DWI scan for the presence or absence of hemorrhage. Hemorrhages were defined as areas of abnormally low signal intensity (hypointense relative to cortical gray matter). A hemorrhagic lesion, when identified, was further characterized by its age and pathogenesis (Table 1). In cases of mixed lesions (such as acute and chronic infarction or hemorrhage), each was analyzed independently. The studies were reviewed retrospectively by a senior neuroradiologist blinded to the clinical data. The b_0 EPI and GRE images from each subject were evaluated at separate sessions in a random order. Subsequently, the b_0 EPI and GRE images were analyzed side-by-side, in conjunction with the DWI scans, for relative conspicuity of hemorrhage and diagnostic certainty (Table 2).

Results of b_0 EPI and GRE imaging were rated as negative, equivocal, or positive for hemorrhage; positive cases were further characterized by pathogenesis or anatomic location. Accuracy of detection of hemorrhage was determined by comparing the blinded interpretations with the formal interpretations of the entire MR or contemporaneous CT study. A case was judged positive for hemorrhage if a contemporaneous CT scan (performed within 2 days) revealed evidence of acute hemorrhage or if MR studies (all sequences) were interpreted as showing evidence of acute hemorrhage. In clinical practice, the MR diagnosis of hyperacute/acute hemorrhage is dependent on the presence of hypointensity on GRE sequences. The GRE se-

Table 1. Number and type of lesions identified on EPI and GRE images

	EPI	GRE	Total
Acute infarction			
Bland			
Heme negative	84	88	88
Heme equivocal	4	0	0
Heme positive	0	0	0
Hemorrhagic			
Heme negative	3	0	0
Heme equivocal	3	0	0
Heme positive	7	13	13
Parenchymal hematoma	8	10	10
SAH	0	2	4
SDH	3	3	3
IVH	5	6	6
Tumor	3	3	3
Chronic infarction			
Bland	2	2	2
Hemorrhagic	2	4	4
Parenchymal hematoma	8	12	12
Petechial hemorrhage	3	30	30
Superficial siderosis	1	7	7
SDH	2	1	1

Note.—EPI indicates b_0 scan from diffusion-weighted echo-planar imaging; GRE, gradient-echo scan; SAH, subarachnoid hemorrhage; SDH, subdural hemorrhage; IVH, intraventricular hemorrhage.

quence therefore served as the standard of reference for detection of hemorrhages, except subarachnoid hemorrhage (SAH), on MR images. Given previous reports documenting the sensitivity of GRE as compared with other MR pulse sequences and CT, and the impossibility of obtaining pathologic correlation in these cases, use of GRE sequences was deemed appropriate.

A binomial test was used to determine whether the difference in hemorrhage detection using EPI and GRE was statistically significant. A P value less than .05 was accepted as statistically significant.

Results

The results of various hemorrhagic lesions are summarized in Table 1. On both GRE and b_0 scans, hemorrhagic lesions, including intraparenchymal hematoma, hemorrhagic infarction, and hemorrhagic tumor, showed decreased signal intensity (Fig 1).

These areas of abnormally decreased signal intensity reflect the T2 dephasing effect induced by paramagnetic blood products. Larger lesions often have heterogeneous signal, with mixed hyperintensity and hypointensity within the lesion core. Analysis of the location of the lesion and its anatomic distribution in conjunction with the composite DWI scans enabled adequate characterization of the lesion's pathogenesis.

A total of 125 cases fulfilled the entry criteria for this study. There were 101 acute infarctions in this series, of which 13 were deemed to be hemorrhagic on the GRE sequence owing to their hypointense signal. Of these, seven (54%) were hypointense on the b_0 image and therefore called hemorrhagic (Fig 1). In three cases, the b_0 image was interpreted as equivocal for hemorrhage, whereas in three cases no hemorrhage was detected (Figs 2 and 3). The difference in sensitivity for detecting hemorrhagic infarction was statistically significant ($P < .05$) (Table 1).

There were 22 acute hematomas with a variety of pathogeneses in various locations, including parenchymal hematomas, subdural or intraventricular hematomas, and hemorrhagic tumors. All were hypointense on the GRE sequences. Nineteen of these lesions were characterized as hemorrhagic (hypointense) on b_0 images, whereas three were not detected.

SAH was detected in two of four cases on GRE scans but it was not detected on any of the b_0 scans (Table 1). In all four cases the presence of SAH was evident on the FLAIR sequence.

Among the cases included in our study, 16 were incidental chronic hematomas (infarction, intraparenchymal, or extraaxial hematomas) all depicted as areas of hypointensity on GRE scans. Ten of these hemorrhages were detected as hypointense lesions on b_0 scans.

Small punctate hemorrhages (microbleeds) or linear cortical staining (gyral hypointensity) indicative of either cerebral amyloid or hypertensive vasculopathy were seen on 37 GRE studies, but only on four of the b_0 examinations (Fig 4). This difference in sensitivity was statistically significant ($P < .001$).

Table 2. Lesion conspicuity and diagnositc certainty with EPI versus GRE

	EPI+/GRE−	EPI>GRE	EPI=GRE	EPI<GRE	EPI−/GRE+
Acute hemorrhagic infarction	0	0	3	7	3
Acute parenchymal heme	0	0	4	6	0
SAH	0	0	0	2	0
SDH	0	0	1	2	0
IVH	0	0	2	3	1
Tumor	0	0	3	0	0
Chronic infarction with heme	0	0	0	3	1
Chronic hematoma	0	0	1	8	3
Petechial hemorrhage	0	0	1	10	19
Gyral hypointensity	0	0	0	5	2

Note.—EPI+/GRE− indicates seen only on EPI; EPI>GRE, seen better on EPI; EPI=GRE, seen equally well on both sequences; EPI<GRE, seen worse on EPI; EPI−/GRE+, seen only on GRE.
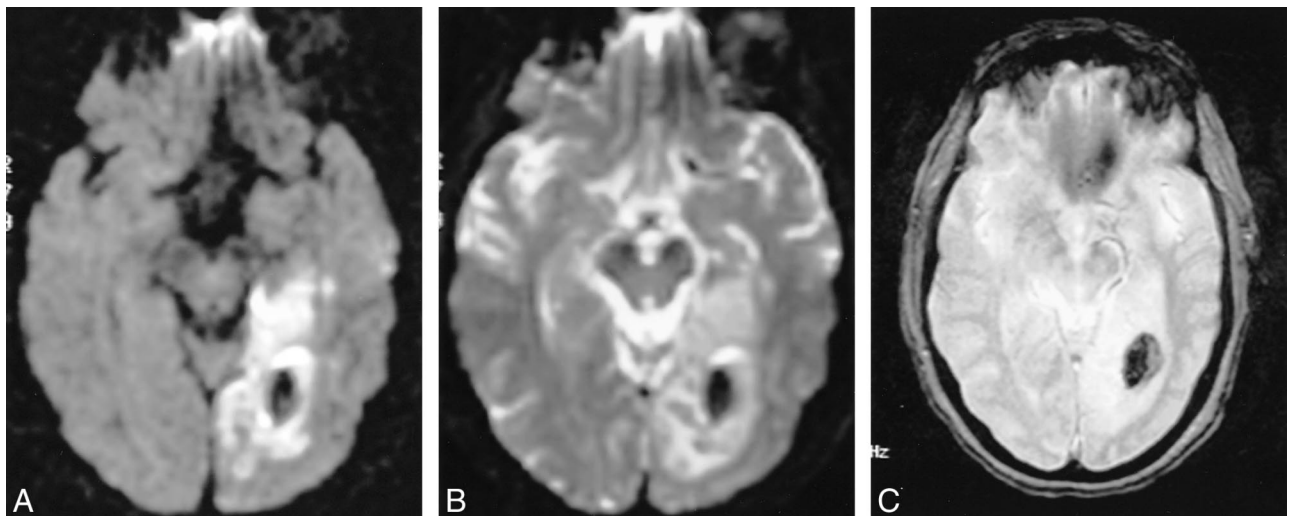
FIG 1.   *A–C,* DWI (10000/102/1, b value of 1000) (*A*), b$_0$ EPI (DWI without diffusion gradients, 10000/102/1) (*B*), and GRE (425/15/1, 20° flip angle) (*C*) MR images of acute hemorrhagic infarction involving the left occipital lobe. The infarction is hyperintense on the DWI scan (*A*) with central hypointensity reflecting hemorrhage. Hypointensity is well depicted on the b$_0$ (*B*) and GRE (*C*) sequences.
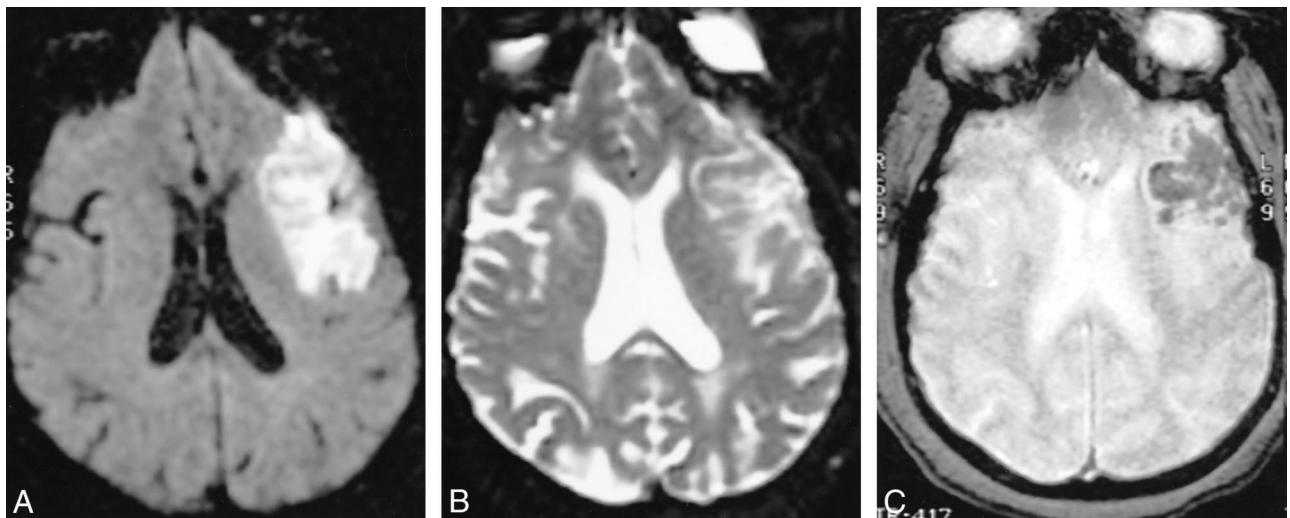

FIG 2.   *A–C,* DWI scan (*A*) shows acute (hyperintense) infarction in the left frontal region. On b$_0$ EPI sequence (*B*) the infarction is relatively hyperintense but somewhat heterogeneous in intensity (scored as negative for hemorrhage on blinded review). The GRE scan (*C*) clearly shows a hypointense hemorrhagic component within the infarction.
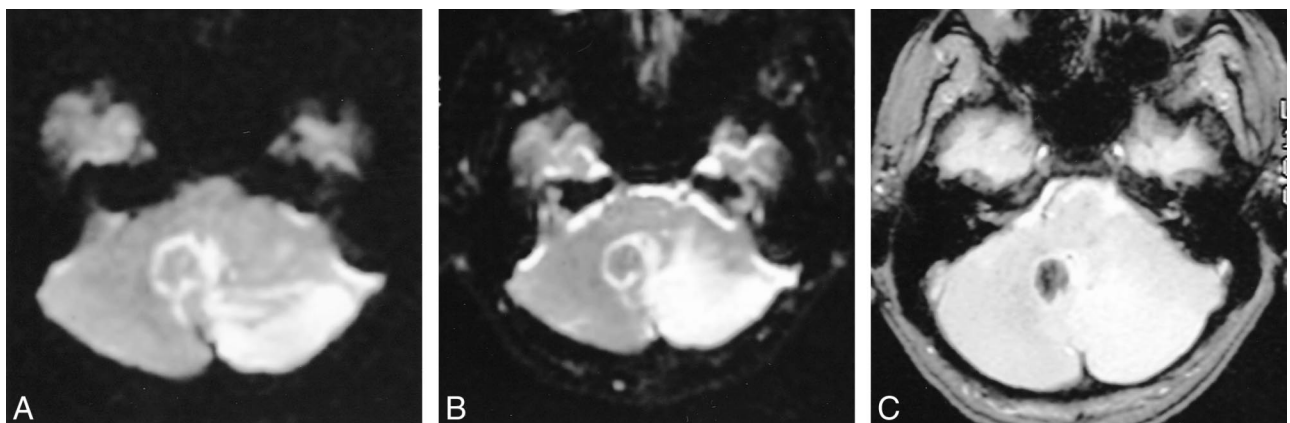

FIG 3.   *A–C,* DWI scan (*A*) shows acute infarction involving the left cerebellar hemisphere, which appears iso- to hyperintense on the b$_0$ EPI scan (*B*). A focus of prominent hypointensity indicative of hemorrhage is seen in the medial portion of the infarction (vermis) on the GRE image (*C*).
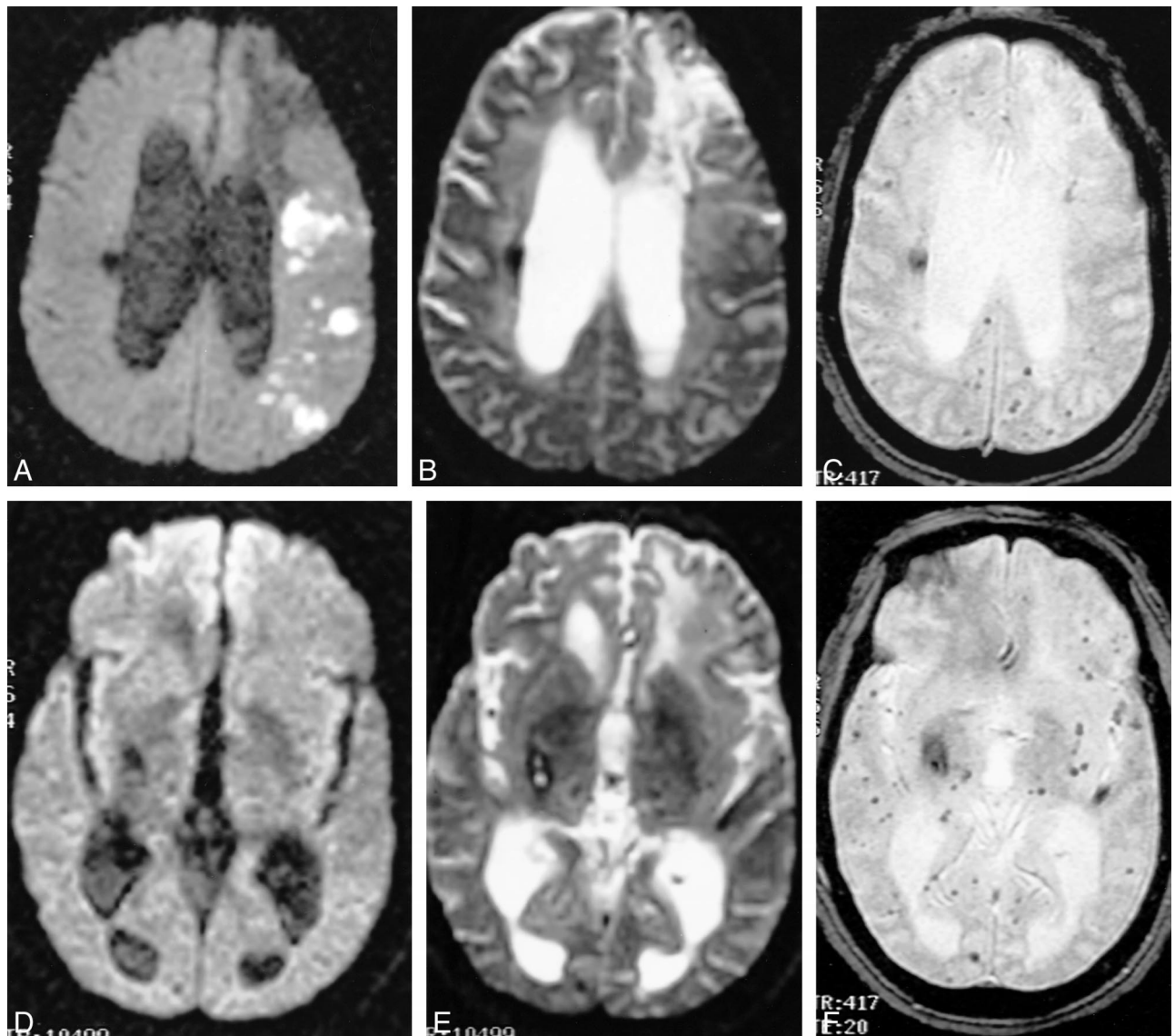
FIG 4. A–C, DWI san (A) at the level of the atria of the lateral ventricles reveals areas of acute (hyperintense) infarction in the frontoparietal region and an area of relative hypointensity due to encephalomalacia in the left frontal lobe. On the b_0 EPI scan (B) the old infarction is hyperintense. Note hypointensity on both the DWI (A) and b_0 EPI (B) scans in the right periatrial region, indicative of chronic hematoma. GRE scan (C) reveals multiple punctate foci of hemosiderin deposition that are not apparent on any other pulse sequences. The right periatrial hematoma is hypointense.

D–F, DWI (D), b_0 (E), and GRE (F) images at the level of the foramen of Monro reveal a chronic right thalamic hematoma, which is hypointense on all pulse sequences; however, the numerous foci of hypointensity are seen only on the GRE scan (F).

Side-by-side analysis of GRE and b_0 images revealed that hemorrhages were invariably more conspicuous on the GRE sequences (Table 2). Acute hematomas in all locations were easily identified on both sequences owing to their hypointense signal; however, in small or subtly hemorrhagic lesions, such as several of the acute infarctions (Figs 2 and 3), the presence of hemorrhage was more readily detected on the GRE scans. In small chronic hemorrhages, the GRE sequence was markedly superior to the b_0 sequence (Fig 4). The overall difference in lesion conspicuity/diagnostic certainty between GRE and EPI scans was statistically significant ($P < .05$).

Discussion

The detection of acute hemorrhage on MR images has been the subject of some controversy. Initially, it was believed that MR imaging was less sensitive than CT in the detection of acute (<24 h) hemorrhage. With increased clinical experience and advances in MR technology, the detection of acute hemorrhage has been facilitated. Over the past several years, a number of clinical human and experimental animal studies have documented that the sensitivity of MR imaging in the detection of intracranial hemorrhage is equal or superior to that of CT (7, 8, 10, 12, 14–21). Moreover, GRE MR sequences are the most sensitive for the detection

of intracranial hemorrhage as compared with other MR sequences (eg, spin-echo T2-weighted) (7–10).

Both b_0 EPI and GRE sequences are sensitive to the susceptibility effects of magnetic field inhomogeneity because they use gradient refocusing pulses. They depict hemorrhages as foci of hypointense signal secondary to proton dephasing. Both sequences have been shown to be superior to fast spin echo, in which the susceptibility effect is minimized by multiple refocusing pulses (10). In a direct comparison of these two sequences, we have found that GRE is more sensitive than b_0 EPI in identifying hemorrhage within acute infarctions. This can be explained in part by the fact that in DWI-EPI, a spin-echo 180° refocusing pulse is applied before the oscillatory gradient pulses, whereas no pulse is used in the GRE sequence (10). Greater contrast resolution is therefore achieved by GRE, allowing for the detection of subtle hemorrhagic lesions that may not be apparent on b_0 EPI (eg, Fig 2). In addition, b_0 EPI fails to provide the same level of diagnostic certainty because of its lower spatial resolution (the matrix is 128^2 as compared with a GRE matrix of 256^2). The lower spatial resolution and lower signal-to-noise ratio of single-shot EPI make the internal architecture of lesions more difficult to characterize, and smaller lesions can be missed. In the infratentorial region and near the base of the skull, b_0 EPI is particularly inferior to GRE owing to the more distinct diamagnetic susceptibility artifacts at the interfaces of tissues with markedly different characteristics.

The findings in series show that the b_0 image from DWI is less sensitive than GRE in revealing acute hemorrhage, in particular in the setting of acute infarction. The poor performance of the b_0 scan may be somewhat skewed by the relatively small sample size (13 hemorrhagic infarctions) as well as by the study design, in which b_0 EPI and GRE scans were interpreted without the benefit of other pulse sequences. On the other hand, this design ensured an unbiased comparison of the sequences, since the majority of the lesions were not hemorrhagic (bland infarctions), thus reproducing the circumstances encountered in clinical practice. Even anecdotal cases of missed or misdiagnosed hemorrhage on b_0 EPI should warrant caution in using this sequence as the primary diagnostic tool in the assessment of hemorrhage. This is important in devising an MR protocol for emergent stroke or trauma. Although DWI-EPI is the fastest and most sensitive sequence in depicting hyperacute/acute cerebral ischemia, GRE appears to be crucial in characterizing the presence or absence of hemorrhage, particularly when thrombolytic therapy is contemplated. In our institution the addition of a GRE sequence adds 2 to 3 minutes to the overall examination time (1:45-minute acquisition). When there are time constraints, or in case of uncooperative, medically unstable, or claustrophobic patients, an ultrafast susceptibility-weighted se-

quence, such as GRE-EPI, may prove useful in reducing imaging time (15).

In depicting chronic hemorrhagic lesions, b_0 EPI is also less sensitive than GRE. In particular, GRE detects the small punctate hemorrhages and linear staining in the cerebral cortex seen in cerebral amyloid angiopathy or hypertensive vasculopathy (16–19), disorders that predominantly affect small vessels (Fig 4). These findings are in agreement with the study by Liang et al (15), who found that GRE-EPI and GRE sequences were much more sensitive than spin-echo EPI or other fast spin-echo sequences in depicting chronic hemorrhage. The GRE-EPI sequence, although faster in acquisition time, was inferior to GRE in detecting infratentorial/skull base lesions, because of susceptibility artifacts and image distortion, and in detecting cortical/subcortical lesions, probably because of image blurring from T2* decay (15).

These small lesions are less conspicuous on b_0 EPI images, most likely as a result of limited spatial resolution. Although these microbleeds are unrelated to the patient's acute clinical presentation, they imply the presence of vascular fragility and a propensity for intracranial hemorrhage (20, 21). No studies have specifically shown that these microbleeds increase the risk of hemorrhagic transformation of infarction, either spontaneous or induced by thrombolytic agents. Nevertheless, identification of these lesions might influence the choice of therapy, since administration of aspirin, anticoagulants, or thrombolytic agents further increases the occurrence of hemorrhage (22).

Both b_0 EPI and GRE sequences are rather insensitive for detecting SAH, which is best depicted on FLAIR images. This result is not unexpected. CSF dilutes SAH and therefore the hematocrit is low. In addition, the oxygen tension is higher than in soft tissues, further lowering the concentration of deoxyhemoglobin. These factors combine to limit the extent of susceptibility effects (23), and the characteristic T2 shortening seen in acute parenchymal hemorrhage is therefore absent in SAH (24). CT remains the standard of reference for evaluating acute SAH, although MR imaging has been reported to offer comparable sensitivity (25, 26), particularly when multiple pulse sequences, including T1-, T2-, proton-density–weighted, and FLAIR (25), are used in combination. In some cases MR imaging has been shown to provide a higher degree of accuracy than CT in depicting SAH (7, 27). Furthermore, various studies have documented greater sensitivity of FLAIR in characterizing subacute and chronic SAH, which may not be apparent on CT studies (28).

Conclusion

GRE is more sensitive and affords greater diagnostic certainty than b_0 EPI in identifying the presence of hemorrhage. Therefore, GRE may be an important pulse sequence in emergency brain MR

studies for acute stroke, especially when thrombolytic therapy is contemplated. In addition to characterizing various acute hemorrhagic lesions, GRE images reveal chronic petechial hemorrhage that is, in the majority of cases, not apparent on b_0 EPI scans. Knowledge of these chronic hemorrhagic lesions may prove in the future to have a clinical implication in choice of therapy.

Acknowledgments

References

 1. Moseley ME, Cohen Y, Mintorovitch J, et al. **Early detection of regional cerebral ischemia in cats: comparison of diffusion- and T2-weighted MRI and spectroscopy.** *Magn Reson Med* 1990;14:330–346
 2. Gonzalez RG, Schaefer PW, Buonanno FS, et al. **Diffusion-weighted MR imaging: diagnostic accuracy in patients imaged within 6 hours of stroke symptom onset.** *Radiology* 1999;210:155–162
 3. Uluğ AM, Beauchamp N, Bryan RN, van Zijl PCM. **Absolute quantitation of diffusion constants in human stroke.** *Stroke* 1997;28:483–490
 4. Beauchamp N, Bryan RN. **Acute cerebral ischemic infarction: a pathophysiologic review and radiologic perspective.** *AJR Am J Roentgenol* 1998;171:73–84
 5. Zimmerman RD, Heier LA, Snow RB, Liu DP, Kelly AB, Deck MDF. **MR imaging feature of acute intracranial hemorrhage studied at 0.5 T with emphasis on sequential intensity changes on multiple pulse sequences.** *AJNR Am J Neuroradiol* 1988;9:47–57
 6. Kelly AB, Zimmerman RD, Snow RB, Gandy SE, Deck MDF. **Head trauma: comparison of MR and CT—experience in 100 patients.** *AJNR Am J Neuroradiol* 1988;9:699–708
 7. Perl JI, Tkach J, Porras-Jamenez M, et al. **Hemorrhage detected using MR imaging in the setting of acute stroke: an in vivo model.** *AJNR Am J Neuroradiol* 1999;20:1863–1870
 8. Patel MR, Edelman RR, Warach S. **Detection of hyperacute primary intraparenchymal hemorrhage by magnetic resonance imaging.** *Stroke* 1996;27:2321–2324
 9. Gustafsson O, Rossitti S, Ericsson A, Raininko R. **MR imaging of experimentally induced intracranial hemorrhage in rabbits during the first 6 hours.** *Acta Radiol* 1990;40:360–368
10. Weingarten K, Zimmerman RD, Deo NV, Markisz J, Cahill PT, Deck MDF. **MR imaging of acute intracranial hemorrhage: findings on sequential spin-echo and gradient-echo images in a dog model.** *AJNR Am J Neuroradiol* 1991;12:457–467
11. Atlas SW, Thulborn KR. **MR detection of hyperacute parenchymal hemorrhage of the brain.** *AJNR Am J Neuroradiol* 1998;19:1471–1477
12. Schellinger PD, Jansen O, Fiebach JB, Hacke W, Sartor K. **A standardized MRI stroke protocol: comparison with CT in hyperacute intracerebral hemorrhage.** *Stroke* 1999;30:765–768
13. Ebisu T, Tanaka C, Umeda M, et al. **Hemorrhagic and nonhemorrhagic stroke: diagnosis with diffusion-weighted and T2-weighted echo-planar MR imaging.** *Radiology* 1997;203:823–828
14. Linfante I, Llinas R, Caplan L, Warach S. **MRI features of intracerebral hemorrhage within 2 hours from symptom onset.** *Stroke* 1999;30:2263–2267
15. Liang L, Korogi Y, Sugahara T, et al. **Detection of intracranial hemorrhage with susceptibility-weighted MR sequences.** *AJNR Am J Neuroradiol* 1999;20:1527–1534
16. Chan S, Kartha K, Yoon SS, Desmond DW, Hilal SK. **Multifocal hypointense cerebral lesions on gradient-echo MR are associated with chronic hypertension.** *AJNR Am J Neuroradiol* 1996;17:1821–1827
17. Good CD, Ng VWK, Clifton A, Britton JA, Hart Y, Wilkins P. **Amyloid angiopathy causing widespread miliary haemorrhages within the brain evident on MRI.** *Neuroradiology* 1998;40:308–311
18. Roob G, Schmidt R, Kapeller P, Lechner A, Hartung HP, Fazekas F. **MRI evidence of past cerebral microbleeds in a healthy elderly population.** *Neurology* 1999;52:991–994
19. Greenberg SM, Finklestein SP, Schaefer PW. **Petechial hemorrhages accompanying lobar hemorrhage: detection by gradient-echo MRI.** *Neurology* 1996;46:1751–1754
20. Roob G, Fazekas F. **Magnetic resonance imaging of cerebral microbleeds.** *Curr Opin Neurol* 2000;13:69–73
21. Fazekas F, Kleinert R, Roob G, et al. **Histopathologic analysis of foci of signal loss on gradient-echo T2*-weighted MR images in patients with spontaneous intracerebral hemorrhage: evidence of microangiopathy-related microbleeds.** *AJNR Am J Neuroradiol* 1999;20:637–642
22. The Stroke Prevention in Reversible Ischemia Trial (SPIRIT) Study Group. **A randomized trial of anticoagulants versus aspirin after cerebral ischemia of presumed arterial origin.** *Ann Neurol* 1997;42:857–865
23. Grossman RI, Kemp SS, Yu IC, et al. **The importance of oxygenation in the appearance of acute subarachnoid hemorrhage on high-field magnetic resonance imaging.** *Acta Radiol* 1986;369:56–58
24. Gomori JM, Grossman RI, Goldberg HI, et al. **Intracranial hematoma: imaging by high field MR.** *Radiology* 1985;157:87–93
25. Chrysikopoulos H, Papanikolaou N, Pappas J, et al. **Acute subarachnoid haemorrhage: detection with magnetic resonance imaging.** *Br J Radiol* 1996;69:601–609
26. Singer MB, Atlas SW, Drayer BP. **Subarachnoid space disease: diagnosis with fluid-attenuated inversion-recovery MR imaging and comparison with gadolinium-enhanced spin-echo MR imaging—blinded reader study.** *Radiology* 1998;208:417–422
27. Noguchi K, Seto H, Kamisaki Y, Tomizawa G, Toyoshima S, Watanabe N. **Comparison of fluid-attenuated inversion-recovery MR imaging with CT in a simulated model of acute subarachnoid hemorrhage.** *AJNR Am J Neuroradiol* 2000:21:923–927
28. Noguchi K, Ogawa T, Seto H, et al. **Subacute and chronic subarachnoid hemorrhage: diagnosis with fluid-attenuated inversion-recovery MR imaging.** *Radiology* 1997;203:257–262